

ORIGINAL ARTICLE

Open Access



Long-term biochar application influences phosphorus and associated iron and sulfur transformations in the rhizosphere

Jiahui Yuan^{1,5}, Hao Chen^{1,2}, Guanglei Chen¹, Prem Pokharel³, Scott X. Chang³, Yujun Wang^{1,2}, Dengjun Wang⁴, Xiaoyuan Yan^{1,2}, Shenqiang Wang^{1,2} and Yu Wang^{1,2*}

Abstract

The effects of long-term biochar application on soil phosphorus (P) flux across the root-soil interface and its availability in the rhizosphere of rice (*Oryza sativa* L) remain unclear. We used diffusive gradients in thin films (DGT), laser ablation-inductively coupled plasma mass spectrometry, and planar optode sensor techniques to characterize, *in-situ*, the 2D heterogeneity and dynamics of rhizosphere soil P, iron (Fe), sulfur (S) and trace element fluxes, dissolved oxygen and pH in paddy soil, after 10 years of biochar application. Compared to the control (no biochar applied), biochar applied at 4.5, 22.5 and 45.0 Mg ha⁻¹ yr⁻¹ decreased rhizospheric P fluxes by 11.6%, 63.4% and 79.0%, respectively. This decrease under biochar treatments was attributed to changed redox status of Fe and S caused by the lower dissolved oxygen in rhizosphere soil and increased soil pH induced precipitating of soluble inorganic P into insoluble P forms, such as calcium-bound and residual P that are unavailable for crop uptake. Higher application rate of biochar resulted in lower As and Pb fluxes in rice rhizosphere and their availabilities for crop uptake. The *in-situ* observation results in rice rhizosphere at μm-scale after 10 years of biochar addition directly showed the complex effects of long-term biochar and rhizosphere heterogeneity on P transformation process.

Highlights

In-situ 2D imaging of rice rhizosphere P, Fe, S, and trace elements was elucidated.

Long-term biochar application conspicuously lowered rice rhizosphere available P.

Soil P release process was related to Fe and S redox status.

Keywords Rice rhizosphere, *In-situ*, High-resolution visualization, Phosphorus availability, Labile iron, Biochar

Handling Editor: Fangbai Li.

*Correspondence:

Yu Wang

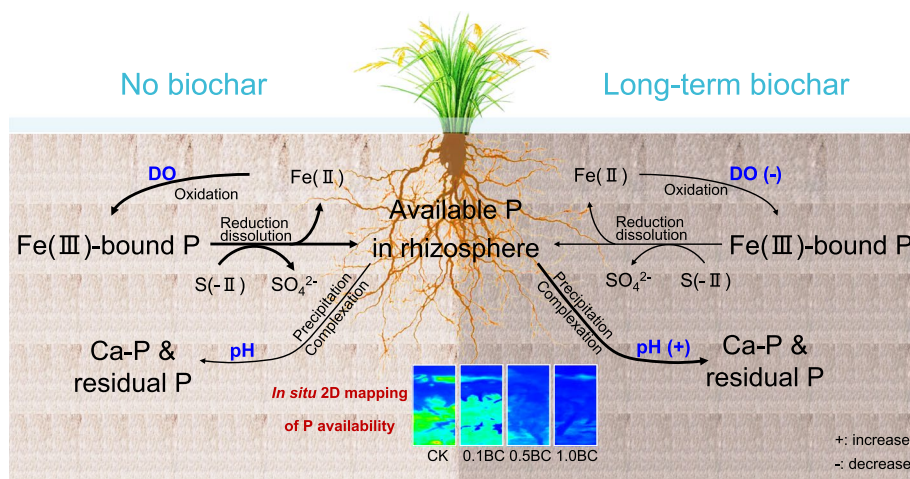
wangyu@issas.ac.cn

Full list of author information is available at the end of the article



© The Author(s) 2024. **Open Access** This article is licensed under a Creative Commons Attribution 4.0 International License, which permits use, sharing, adaptation, distribution and reproduction in any medium or format, as long as you give appropriate credit to the original author(s) and the source, provide a link to the Creative Commons licence, and indicate if changes were made. The images or other third party material in this article are included in the article's Creative Commons licence, unless indicated otherwise in a credit line to the material. If material is not included in the article's Creative Commons licence and your intended use is not permitted by statutory regulation or exceeds the permitted use, you will need to obtain permission directly from the copyright holder. To view a copy of this licence, visit <http://creativecommons.org/licenses/by/4.0/>.

Graphical Abstract



1 Introduction

Production of biochar from crop residues is an important method of agricultural waste management, and biochar application to agricultural land helps increase soil organic matter and nutrients availability such as nitrogen and phosphorus (P) for crop uptake (Wang et al. 2023; Pan et al. 2021). The efficacy of biochar application in soil P availability had more pronounced beneficial effects observed in short-term pot or incubation experiments, contrasting with weakened effects in long-term field conditions (Gao et al. 2019; Glaser and Lehr 2019). Previous studies are more focused on the bulk soil, while biochar-root interaction in the rhizosphere zone has often been neglected, despite it being the most active and dynamic region of nutrient cycling and an important source and sink of P for crop and soils (Apori et al. 2021; Shen et al. 2011). Assessment of rhizosphere P cycling is thus needed for in-depth understanding on how biochar influences nutrient availability for crop uptake.

The rice rhizosphere emerges as a pivotal zone for soil P transformation and crop P uptake. Therefore, it is important to investigate the availability of P in the soil within the rhizosphere, as it directly influences the release process of P in this zone. The complexity and heterogeneity of the rhizosphere environment induced by the release of root exudates, root release of oxygen and rhizosphere microbial activity have potential implications for soil P availability (Yin et al. 2020; Wei et al. 2019). The fluctuation in oxygen levels significantly affects soil P cycling, and the radial oxygen loss is conducive to the changes in the microscale redox potential (Larsen et al. 2015), which further change soil P availability. The migration

and transformation of soil P are mainly controlled by its interaction with elements like iron (Fe) and sulfur (S) and arsenic (As) in flooded paddy soils. These interactions occur mainly in the rhizosphere zone where the redox potential of Fe and S undergo changes due to the utilization of dissolved oxygen (DO) during the decomposition of organic matter (Li et al. 2021), influence adsorption and fixation of P and make it less accessible for uptake by plants (Weihrach and Opp 2018). The dissolution of P from Fe(III)-bound P is a primary source of available P in flooded paddy soils (Khan et al. 2019; Maranguit et al. 2017; Zhang et al. 2003), which might be via the sulfide-induced reduction of Fe(III) hydroxide and direct microbial Fe(III) reduction (Brodersen et al. 2017). Moreover, the speciation and concentration of As is influenced by the extent of Fe(III) reduction and competitive adsorption with P (Deng et al. 2020). In a flooded paddy soil with a high microbial Fe reduction potential, microbial sulfate reduction decreased As mobilization by its precipitation or sorption with FeS minerals (Xu et al. 2019), and the variations in interactions between Fe and P triggered by fluctuations of redox conditions and root activities, which further explains solute release patterns/mechanisms (Fang et al. 2021a). Furthermore, apart from the interaction of soil P with these elements, lower soil pH in rice rhizosphere plays a crucial role in increasing soil P mobilization by the dissolution of calcium phosphate (Brodersen et al. 2017; Marschner et al. 2011).

The distribution of P in rice rhizosphere is heterogeneous on the millimeter scale (Larsen et al. 2015). Challenges in precisely assessing this process in the rhizosphere have been attributed to sampling and

interpretative constraints. Traditional rhizosphere research methods including soil shaking, root rinsing, and root bag approaches involve destructive sampling, and low-resolution of nutrient cycling quantification (Kreuzeder et al. 2018; Brodersen et al. 2017). To address these challenges, the diffusive gradients in thin films (DGT) method, characterized by its *in-situ*, high-resolution, and multi-parameter features based on simple diffusion principles, offers a promising solution (Yin et al. 2020; Williams et al. 2014). The utilization of this methodology by Fang et al. (2021a, b) revealed that rice rhizosphere P depletion facilitated phosphatase activities and mineralization of organic P, which further contributed to a deeper comprehension of P cycle in paddy soils. Our recent research on rice rhizosphere soil P and Fe distribution also demonstrated the successful application of DGT technique in studying nutrient cycling in the paddy soil (Wang et al. 2021a, b; Wang et al. 2019). However, to achieve a comprehensive understanding, concurrently measurement of labile P flux and key factors influencing P release from rhizosphere soil becomes imperative.

The addition of biochar generally improves soil P availability. This improvement primarily stems from the dissolution of P from the biochar material, the increased reduction and dissolution of P in Fe(III) hydroxide, and mineralization of soil organic P by promoting the activities of microorganisms or phosphatase (Eltohamy et al. 2023; Yang et al. 2021; Zhou et al. 2020). However, the conflicting results could potentially be caused by the immobilization of P through the adsorption or precipitation (Yang et al. 2019; Chintala et al. 2014) caused by an elevation in soil pH and crop uptake (Xu et al. 2016). Moreover, the impact of biochar on soil P availability varies depending on the timeframe since its application; the effect is large in the short-term (< 1 year) pot or incubation experiments but weakens in the long-term (> 1 year) field conditions (Gao et al. 2019; Glaser and Lehr 2019). A four-year-long field study in paddy field illustrated that the effectiveness of biochar in increasing soil P availability decreased with the increase in application rate and time (Jiang et al. 2021). It will thus be valuable to understand the mechanism of long-term biochar effects on soil P availability. Notably, prior studies have tended to focus more on soil processes and less on rhizosphere processes. In our investigation using the DGT technique, we discovered a significant reduction in rice rhizosphere available P after 9 years of biochar addition in the field (Chen et al. 2022). However, the lack of available data on long-term effects of biochar on nutrient cycling, particularly in the rhizosphere zone, has been limiting our ability to include biochar amendment as one of the best management practices on a broad scale across the globe (Wei et al. 2019).

Herein, based on previous study, the present study employed a combined *in-situ* high-resolution approach to delve deeply into the effects of 10 years of continuous biochar application on the bioavailability of soil P, elucidating the key processes influencing P release in the rhizosphere zone of rice, by using a pot experiment. The main hypotheses of this research include: 1) the application of biochar can change the availability of P, Fe, S and trace elements in the rhizosphere of rice; and 2) biochar application affects Fe and S cycles through altering DO and pH, and thereby changing the P availability in the rice rhizosphere soil. The results provide intuitive information on rhizosphere microscale for the sustainable utilization of agricultural waste resources.

2 Materials and methods

2.1 Soil and biochar

The soil was obtained from the upper 20 cm of soil profile in an agricultural land, where biochar had been applied continuously at different rates for 10 years in a rice–wheat cropping experiment, at the Yixing Agro-Environment Research Base of the National Agroecosystem Observatory and Research Station of Changshu (YX, 119°54′E, 31°16′N). The field experiment had four treatments: 1) no biochar applied (control, CK); 2) biochar applied at 0.1% of soil weight (0.1BC, 4.5 Mg ha⁻¹ yr⁻¹); 3) biochar applied at 0.5% of soil weight (0.5BC, 22.5 Mg ha⁻¹ yr⁻¹); and 4) biochar applied at 1.0% of soil weight (1.0BC, 45.0 Mg ha⁻¹ yr⁻¹). In all treatments, the chemical P fertilizers were added at 60 kg P₂O₅ ha⁻¹ in each season. The urea and potassium chloride (KCl) application doses were 250 kg N ha⁻¹ (in a ratio of 3:4:3 at basal, tillering, and jointing stages) and 60 kg K₂O ha⁻¹, respectively. Detailed information on biochar, soil and fertilization methods used in the field experiment can be found in Chen et al. (2022). The biochar used in the field was derived from rice straw and produced through pyrolysis at a temperature of 500 °C for 8 h, with a heating rate of 5 °C min⁻¹. It was then thoroughly mixed with the top 0–20 cm layer of soil. The properties of biochar were as follows: pH 9.16, total organic carbon and nitrogen concentrations of 620 and 13.3 g kg⁻¹, the cation exchange capacity of 18.9 cmol kg⁻¹, and the concentrations of Ca, P, K, Na, Mg, Fe, Mn, Cu and Zn extracted by Mehlich III which were 2.63, 1.06, 18.43, 3.94, 1.41, 0.01, 0.55, 0.0016 and 0.05 g kg⁻¹, respectively. Soil samples were collected from three random points within each plot using an auger after wheat harvest, and then was composited for each plot. Each soil sample was mixed well and processed separately by removing stones and visible roots, air-drying, and sieving through a 2 mm mesh. A portion of the processed soil was used to characterize soil basic properties and the remaining soil was used in a pot experiment.

Soil Olsen-P concentrations were 32.4, 25.9, 29.3 and 37.0 mg kg⁻¹, for the CK, 0.1BC, 0.5BC and 1.0BC treatments, respectively.

2.2 Greenhouse experiment

A greenhouse experiment was conducted using rice seedlings in custom-designed Perspex rhizoboxes from July 27 to August 26, 2020. Each rhizobox had dimensions of 10×8×20 cm³ and included a detachable plate. The soil used in the experiment was collected and processed separately for each plot in the field experiment. A total of 1 kg (oven-dry equivalent) of air-dry soil was filled into each rhizobox after pre-incubation at 70% water-holding capacity for one week. Rice seedlings were produced in a nursery. Two 10-day-old rice seedlings with a pruned root length of 1.5 cm were transplanted to each rhizobox near the detachable plate. To prevent light penetration into the soil and roots, the rhizoboxes were wrapped with tin foil and kept inclined at 30° angle, allowing the roots to grow along the side of the detachable plate. After transplanting the rice seedlings, nitrogen and potassium fertilizers were added to the soil. Base fertilizers consisted of 0.200 g urea kg⁻¹ soil and 0.175 g KCl kg⁻¹ soil. Two weeks after transplanting, a topdressing of 0.100 g urea kg⁻¹ soil was applied. The soils were flooded with 3 to 5 cm of water covering the soil surface during the whole experiment.

2.3 Planar optode sensor imaging

Soil pH and DO concentrations in the soil solution were measured using a planar optode sensor (PO2100, EasySensor Ltd. Nanjing, China) 14 and 28 days after transplanting. Refer to Supporting Information Text S1 for detailed procedural steps.

2.4 Zr-oxide DGT imaging

Horizontal and vertical distributions of soil DGT-labile P around root tips were visualized on a submillimeter scale using a Zr-oxide DGT (EasySensor Ltd. Nanjing, China) 14 and 28 days after seedling transplanting. Refer to Supporting Information Text S2 for detailed procedural steps. The scheme of experimental design is shown in Fig. S1.

2.5 HR-ZCA DGT imaging

The fluxes of sulfides, metallic cations and oxyanions (P, S, Fe, As, Pb, Co, Ni, Cu and Zn) in the rhizosphere soil were determined after 30 days of transplanting, using HR-ZCA DGT imaging (EasySensor Ltd. Nanjing, China) followed by laser ablation-inductively coupled plasma mass spectrometry (LA-ICP-MS, Agilent Technologies 7700, USA). Refer to Supporting Information Text S3 for detailed procedural steps.

2.6 Soil P fractionation

Soil P fractions were analyzed on samples collected 30 days after transplanting of seedlings following the Tieszen method (Tiessen and Moir 1993). Refer to Supporting Information Text S4 for detailed procedural steps.

2.7 Data analysis

The 2D imaging for measuring the DO concentration, soil pH and selected elements in the rhizosphere was mapped using the Origin software. The association among the elements studied under different biochar application rates was explored through principal component analysis (PCA) by Origin software. Pearson correlation analysis exploring the linear relationship between the selected elements was presented as correlation diagram performed through R version 3.6.1.

3 Results and discussion

3.1 Distribution and dynamics of labile P, DO and pH in rhizosphere

The 2D imaging of the soil rhizosphere P flux illustrated an obvious P depletion area around root tips regardless of the treatment, with the low DGT-P flux corresponding to the area of soil P depletion; the P depletion area gradually expanded with the rice growth as shown from the measurements made 14 and 28 days after the transplanting of seedlings (Fig. S2). High heterogeneity of the localized rhizosphere environment indicated the variations induced by the roots of rice seedlings under different treatments (Fig. S2). The longest root length and total root length were highest in 0.5BC treatment (Table S1). In contrast to previous *ex-situ* studies by Jin et al. (2019), this study with *in-situ* high-resolution imaging demonstrated that biochar application reduced P availability in rice rhizosphere soil. Compared with CK treatment, P flux was decreased by 11.6%, 63.4% and 79.0% under the 0.1BC, 0.5BC and 1.0BC treatments, respectively (Fig. S3). The 2D imaging of DO and soil pH also showed highly heterogeneous effects of the treatments in the rhizosphere (Fig. S2). Oxygen secretion was observed along all visible roots and increased over time. The amount of DO increased towards the root tips which corresponds to the increase in root density and greater accumulation of oxygen from root respiration. Labile P decreased with increasing biochar application rate on both measurement times, indicating a negative impact of biochar on rhizospheric P flux.

To further elucidate the correlations, labile P and DO measurements at the same position (2×4 cm²) were compared and the average values of unit resolution in the vertical direction for 14th and 28th day measurement were calculated (Fig. 1). The P depletion area around root was positively related with the area of high

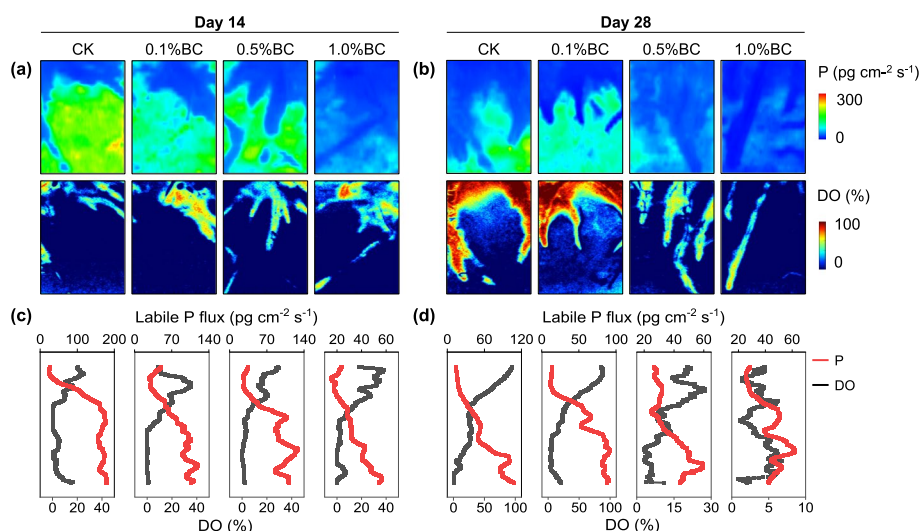


Fig. 1 Temporal and spatial variations of labile P flux and dissolved oxygen (DO) analyzed by 2D imaging of Zr-oxide DGT and planar optode sensor. Dynamics of labile P flux and DO level at the same rice rhizosphere location ($2 \times 4 \text{ cm}^2$) on the 14th (a) and 28th day (b) after the transplanting of seedlings. Variations in labile P flux against DO level in rhizosphere on the 14th (c) and 28th day (d) after seedling transplanting. The P flux and DO increased with the color scale shown from blue to red. CK, 0.1BC, 0.5BC and 1.0BC refer to biochar application rates of 0%, 0.1%, 0.5% and 1% of soil weight which are equivalent to 0, 4.5, 22.5 and 45.0 $\text{Mg ha}^{-1} \text{ yr}^{-1}$ respectively

DO. Consistent with previous studies, soil labile P had the lowest flux when DO concentration was the highest, which indicated the primary effect of root oxygen secretion and nutrient uptake process (Fang et al. 2021a; Williams et al. 2014). In the vertical profile, labile P flux showed a narrower horizontal spread in the treatments with higher rate of biochar application

on 14th and 28th days of measurement (Fig. 1c and 1d). Labile P flux and DO had a negative relationship across all treatments. The correlation was gradually weakened along the rate of biochar application. The root-regulated variation of soil pH was weaker than that of labile P, regardless of the treatment and time of measurement (Fig. 2a and b). Soil pH was significantly increased with

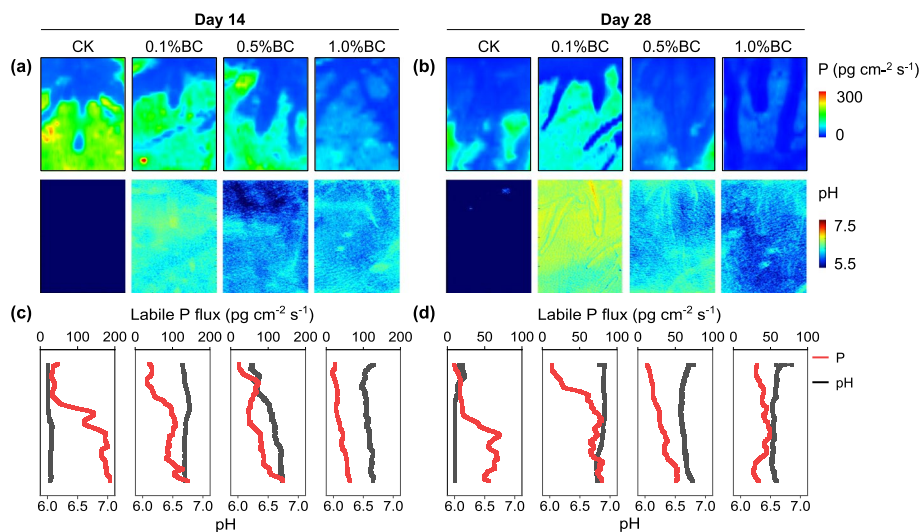


Fig. 2 Temporal and spatial variations of labile P flux and pH analyzed by 2D imaging of Zr-oxide DGT and planar optode sensor. Dynamics of labile P flux and pH level at the same rice rhizosphere location ($2 \times 4 \text{ cm}^2$) on the 14th (a) and 28th day (b) after the transplanting of seedlings. Variations in labile P flux against pH level in rhizosphere on the 14th (c) and 28th day (d) after seedling transplanting. The P flux and pH increased with the color scale shown from blue to red. CK, 0.1BC, 0.5BC and 1.0BC refer to biochar application rates of 0%, 0.1%, 0.5% and 1% of soil weight which are equivalent to 0, 4.5, 22.5 and 45.0 $\text{Mg ha}^{-1} \text{ yr}^{-1}$ respectively

increasing biochar application rate. The vertical distribution profile of labile P plotted against soil pH (Fig. 2c and d) showed a weak correlation regardless of treatment and time of measurement, unlike its strong negative correlation with DO.

The difference in labile P flux along the vertical axis in the rhizosphere across all the treatments can be attributed to plant uptake of labile P, microbial immobilization and the adsorption of P by Fe plaques on the root surface (Fang et al. 2021a). The oxygen secreted by roots induces changes in redox conditions of the soil solution in the rhizosphere that further affects soil P availability for plant uptake and microbial metabolism (Larsen et al. 2015). Under anaerobic condition (i.e. low DO), bacterial demand for P decreases, and the activity of Fe-reducing bacteria increases to enhance labile P flux in rice rhizosphere (McRose and Newman 2021; Wang et al. 2021a, b). The fluctuation of redox potential affects the release process of P through Fe cycle (Yuan et al. 2021, 2020). Since the region of redox fluctuation is narrower than that of P diffusion around root surfaces, the labile P flux gradient among the treatments was associated with plant uptake of labile P and the formation of Fe plaques on root surfaces (Fang et al. 2021a). Additionally, the fact that root uptake of labile P by mass flow occurs faster than the rate of labile P diffusion from soil solution to rhizosphere (Khan et al. 2019), suggesting that plant uptake of labile P was the main driving factor for the reduction of soil available P in the rhizosphere.

The high specific surface area of biochar, along with presence of alkaline cations (Ca^{2+} and Mg^{2+} , for instance) in biochar promoted the adsorption and precipitation of soil P (Ghodsad et al. 2022, 2021), thereby reducing soil P availability. The P fraction data showed that Ca-P and residual P increased with the increasing biochar application rate (Fig. S4). The biochar used in this study was pyrolyzed at high temperature (500 °C) and contained a high amount of Ca^{2+} and Mg^{2+} ions, which significantly contributed to the adsorption of P (Borno et al. 2018; Ngatia et al. 2017). The adsorption of P on biochar surface occurs by the exchange between solution anions of P and oxidizing functional groups present on biochar surfaces (Chintala et al. 2014). Yang and Lu (2022) have shown that the effect of biochar addition on P availability varied with growth stages of rice that were linked to variations in soil pH and crop uptake of P. In this study, biochar application resulted in an increase in soil pH, which might affect soil P availability through biogeochemical processes, including adsorption–desorption, dissolution, precipitation and complexation (Eduah et al. 2019). However, as soil pH was not strongly affected by biochar application rates, labile P flux was more linked to the change in crop uptake of P and soil DO.

3.2 Distribution of and relationships between labile P, Fe, S and trace elements in rice rhizosphere

Consistent with previous findings (Fang et al. 2021b; Yin et al. 2020; Williams et al. 2014), rice roots substantially affected the availability of P, Fe and S (Fig. 3). Two possible reasons for the heterogeneity of distribution of these elements in the rhizosphere on the vertical axis are the variation in adsorption and secretion of these elements by rice roots, and the drastic change in physicochemical conditions in the microenvironment of the rice rhizosphere. The decrease in P and Fe flux was expanded further away from the root surface (Fig. 3). This indicates that the effect of Fe plaque formation on rice root surface (Fig. S6) was caused by root oxygen secretion on rhizosphere P adsorption and fixation (Wang et al. 2019). Furthermore, the presence of Fe plaques on root surfaces might be the main factor contributing to the decrease in fluxes of As and Pb in rice rhizosphere, as a significant positive relationship was observed between them (Fig. 4a and b). In contrast to previous findings (Fang et al. 2021b; Yin et al. 2020; Williams et al. 2014), no apical Fe flux hotspots were observed in our study (Fig. 3). This might be owing to the fact that oxidative immobilization of Fe by root oxygen secretion was stronger than the reductive dissolution of Fe by Fe-reducing bacteria activity. Moreover, the spatial patterns of labile P and trace elements (As, Pb, Co, Ni, Cu and Zn) in rhizosphere were congruent with root distribution (Fig. 3 and S5). The average flux of S, labile P and trace elements including Fe, As and Pb was lower in rice rhizosphere compared to bulk soil, and was generally decreased by the application of biochar. Biochar played a significant role in affecting the intensity of trace element fluxes but did not exhibit any patterns in their spatial distribution. Among the trace elements studied, substantial As flux was observed in the rhizosphere but not in bulk soil, while Co and Ni fluxes were lower in rhizosphere compared to bulk soil, and increased with higher rates of biochar application (Fig. S5). Unlike Co, the flux of Cu was greater in the rhizosphere compared to the bulk soil zone (Fig. S5).

The results of PCA highlight distinct differences in flux characteristics among the treatments (Fig. 4a). Soil Fe, S, As and Pb had significantly positive relationships with P ($p < 0.01$) (Fig. 4b), of which the strongest positive relationship was between P and Fe (correlations coefficients of 0.87, $p < 0.001$) and the next between P and S (correlations coefficients of 0.69, $p < 0.001$; Fig. 4c), further emphasizing the importance of Fe and S cycles in soil P mobilization. The microbial and chemical process-mediated Fe(III) reduction in anaerobic conditions of paddy soil enhanced the desorption and dissolution of P from Fe(III) hydroxide (Khan et al. 2019). The significant linear correlation between dissolved sulfide

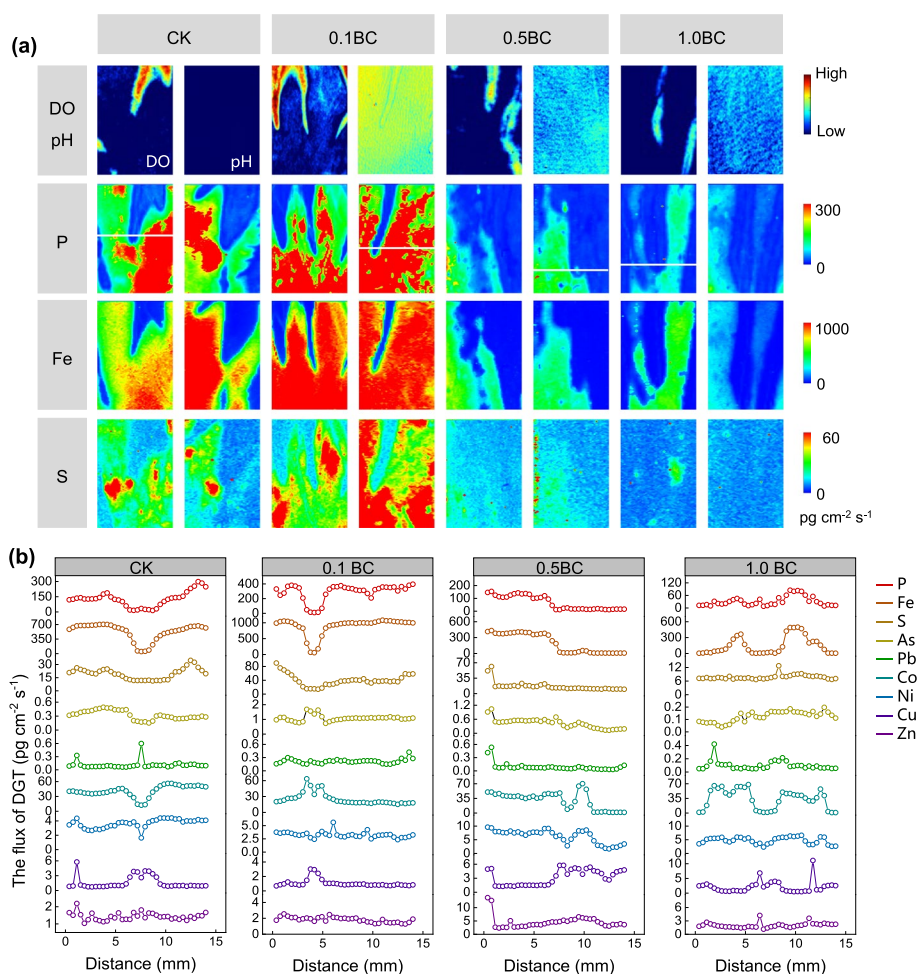


Fig. 3 Characteristics of DO pH and labile P Fe and S fluxes measured by 2D imaging of planar optode sensor and HR-ZCA DGT after ten years biochar application. **(a)** Characteristics of labile P Fe and S fluxes and DO pH level in rice rhizosphere ($1.4 \times 1.6 \text{ cm}^2$) on the 30th day after the transplanting of seedlings. In the first row there were DO on the left and pH on the right in each treatment and the last few rows represented the fluxes of P Fe and S at the same rhizosphere position as DO or pH. The flux increased with the color scale shown from blue to red. The white line location was selected as the root tip position to analyze the correlation between the subsequent elements. **(b)** Variations in labile P and various elements fluxes in rice root tip zone along the white line in **(a)**. CK, 0.1BC, 0.5BC and 1.0BC refer to biochar application rates of 0%, 0.1%, 0.5% and 1% of soil weight which are equivalent to 0, 4.5, 22.5 and 45.0 $\text{Mg ha}^{-1} \text{ yr}^{-1}$ respectively

and labile P indicated that the migration of P is mainly regulated by reduction and dissolution of Fe(III)-bound P triggered by sulfide and the mineralization of organic carbon related to sulfate reduction (Wu et al. 2019). The Fe(III) hydroxide and sulfate are reduced to Fe(II) and S(-II) under flooded anaerobic conditions. Biochar application has been shown to promote Fe(III) hydroxide and sulfate reduction by increasing soil organic carbon content (Rajendran et al. 2019). Biochar can also act as an electron shuttle, promoting microbial reduction of Fe(III) (Kappler et al. 2014). In our study, the decrease in labile S(-II) flux may be attributed to the formation of S(-II) precipitates by sulfate reduction, which further affects the adsorption of soil phosphate. Additionally, the

formation of Fe(II) phosphate under reducing conditions also resulted in a decrease in soil P availability (Wu et al. 2021). The biogeochemical processes of elements like Fe and S can regulate the change of redox activity regulated by the roots of rice in flooded conditions. These biogeochemical processes play a crucial role in regulating soil P availability in rice rhizosphere under variable rates of biochar application. Therefore, this supports our second hypothesis that biochar application affects Fe and S cycles by altering DO and pH, subsequently influencing soil P bioavailability in rice rhizosphere.

The fluxes of Cu and Ni were significantly negatively correlated with S(-II) in the rhizosphere. The increase in their flux in the rhizosphere was due to S oxidation

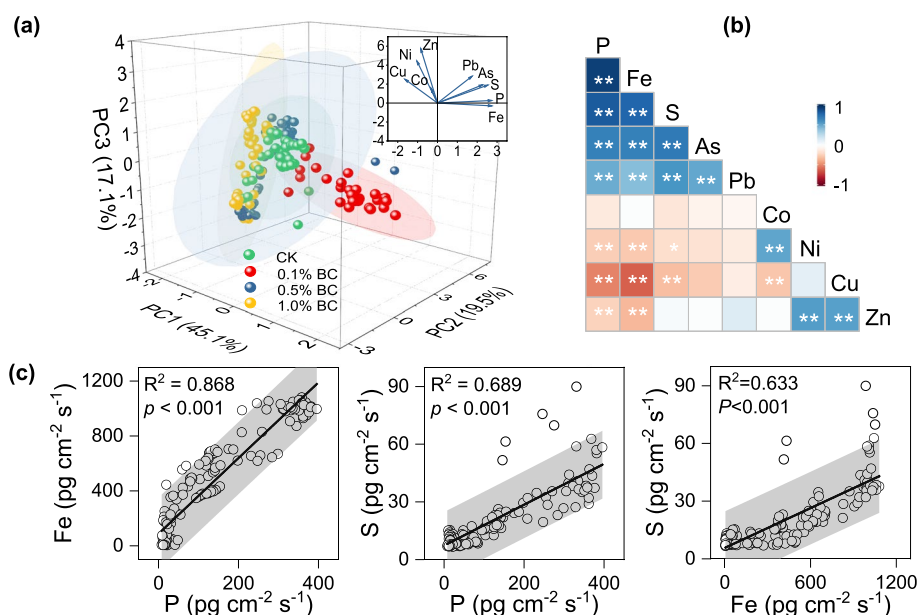


Fig. 4 Relationships between elements in rice root tip zone. Principal components analysis plot (a) and correlation diagram (b) of elements in rice root tip zone under different biochar application rates. (c) The linear regression relationships between P Fe and S in rice root tip zone. CK, 0.1BC, 0.5BC and 1.0BC refer to biochar application rates of 0%, 0.1%, 0.5% and 1% of soil weight which are equivalent to 0, 4.5, 22.5 and 45.0 Mg ha⁻¹ yr⁻¹ respectively. The gray shaded area represents 95% confidence interval. * represents significance at $p < 0.05$ and ** represents significant at $p < 0.01$

(Kreuzeder et al. 2018). Under reducing conditions, the formation of sulfide precipitate (such as CuS) may also reduce their fluxes. Significant negative correlations of Cu and Ni with Fe (Fig. 4b) indicate that the adsorption of Cu and Ni by roots was impacted by the formation of Fe plaques on root surfaces, as Fe plaques act as a barrier for their adsorption. A coupling-decoupling phenomenon between Ni and Fe at different positions was found

in the rhizosphere of aquatic plants (Li et al. 2022). Root-induced oxidation and acidification in soil solution can improve the availability of Ni, however, the formation of Fe plaques resulting from oxidation may reduce Ni mobility through adsorption. Moreover, a clear relationship among Co, Ni, Cu and Zn was observed by PCA, highlighting the crucial role of biochar in influencing trace element availabilities (Figs. 4a and 5). These findings were

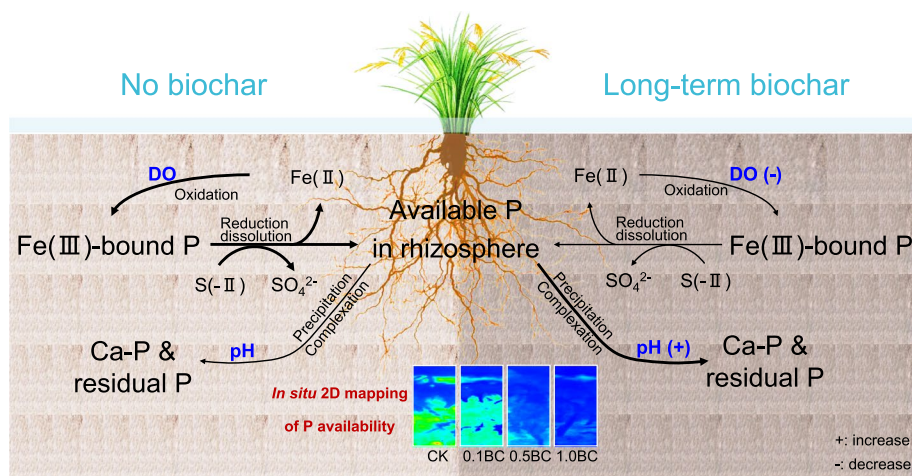


Fig. 5 The conceptual diagram of P release processes in rice rhizosphere with or without long-term biochar application (10 years). The thickness of the arrows indicates the main process that occurs under different treatments. The + and - signs indicate increase and decrease respectively in pH and dissolved oxygen (DO). The P flux increased with the color scale shown from blue to red. CK, 0.1BC, 0.5BC and 1.0BC refer to biochar application rates of 0%, 0.1%, 0.5% and 1% of soil weight which are equivalent to 0, 4.5, 22.5 and 45.0 Mg ha⁻¹ yr⁻¹ respectively

similar to the results of previous study that used different DGT substrates in determining the availability of trace elements (Yin et al. 2020).

4 Conclusion

Here, we clarified how to reduce P availability in the rhizosphere zone after 10 years of biochar application on paddy soil. We attribute these findings to DO-derived morphological changes of redox-active elements (Fe and S) and pH-triggered transformation of Ca-P and residual P. The spatial distribution similarity of P, Fe and S proves evidence that variation in root-mediated redox-active element morphology regulates P transformation and release processes in paddy soil. The consistency of chemical flux in spatial distribution characteristics and its difference under biochar addition directly illustrate the complexity of how biochar affects the interaction among elements. Combined with our previous research results, biochar not only increased soil Ca-P but also promoted the hydrolysis of organic P due to the stimulation of phosphatase activity, which eventually could maintain soil available P at sufficient level for crop uptake. Therefore, biochar can be regarded as a slow-release P fertilizer due to its sustained-release effect on soil P by affecting biochemical processes related to P transformation. However, it is crucial to note that a high biochar application rate may lead to soil P accumulation due to the elevated P content in biochar. The ability to adjust the biochar application rate and chemical P fertilizer becomes imperative in addressing this issue. This will help us further realize and utilize biochar resource more efficiently in agricultural eco-system.

Supplementary Information

The online version contains supplementary material available at <https://doi.org/10.1007/s44246-024-00109-0>.

Supplementary Material 1

Acknowledgements

Not applicable.

Authors' contributions

All authors contributed to the study conception and design. Material preparation, data collection and analysis were performed by Jiahui Yuan, Hao Chen and Guanglei Chen. The first draft of the manuscript was written by Jiahui Yuan and all authors commented on previous versions of the manuscript. All authors read and approved the final manuscript.

Funding

This work was funded by the Natural Science Foundation of Jiangsu Province (BK20230049), the National Natural Science Foundation of China (No. 42277026), the Jiangsu Agricultural Science and Technology Innovation Fund (CX(22) 3200), and Jiangsu Modern Agricultural Machinery Equipment and Technology Demonstration Promotion Project (NJ2023-29).

Availability of data and materials

The data generated during and/or analyzed during the current study are available from the corresponding author upon reasonable request.

Declarations

Competing interest

Scott X. Chang, Yujun Wang, and Xiaoyuan Yan are editorial board members for Carbon Research and were not involved in the editorial review, or the decision to publish, this article. All authors declare that there are no competing interests.

Author details

¹State Key Laboratory of Soil and Sustainable Agriculture, Changshu National Agro-Ecosystem Observation and Research Station, Institute of Soil Science, Chinese Academy of Sciences, Nanjing 210008, China. ²University of the Chinese Academy of Sciences, Beijing 10049, China. ³Department of Renewable Resources, University of Alberta, Edmonton, AB, Canada. ⁴School of Fisheries, Aquaculture and Aquatic Sciences, Auburn University, Auburn, AL 36849, USA. ⁵Heilongjiang Academy of Black Soils Conservation and Utilization, Key Laboratory of Black Soil Protection and Utilization, Ministry of Agriculture and Rural Affairs, Heilongjiang Academy of Agricultural Sciences, Harbin 150086, China.

Received: 9 November 2023 Revised: 7 February 2024 Accepted: 14 February 2024

Published online: 11 March 2024

References

- Apori SO, Byalebeka J, Murongo M, Ssekandi J, Noel GL (2021) Effect of co-applied corn cob biochar with farmyard manure and NPK fertilizer on tropical soil. *Resources Environment and Sustainability* 5:100034. <https://doi.org/10.1016/j.resenv.2021.100034>
- Borno ML, Muller-Stover DS, Liu FL (2018) Contrasting effects of biochar on phosphorus dynamics and bioavailability in different soil types. *Sci Total Environ* 627:963–974. <https://doi.org/10.1016/j.scitotenv.2018.01.283>
- Brodersen KE, Koren K, Mosshammer M, Ralph PJ, Kuhl M, Santner J (2017) Seagrass-mediated phosphorus and iron solubilization in tropical sediments. *Environ Sci Technol* 51(24):14155–14163. <https://doi.org/10.1021/acs.est.7b03878>
- Chen H, Yuan JH, Chen GL, Zhao X, Wang SQ, Wang DJ, Wang L, Wang YJ, Wang Y (2022) Long-term biochar addition significantly decreases rice rhizosphere available phosphorus and its release risk to the environment. *Biochar* 4(1). <https://doi.org/10.1007/s42773-022-00178-7>
- Chintala R, Schumacher TE, McDonald LM, Clay DE, Malo DD, Papiernik SK, Clay SA, Julson JL (2014) Phosphorus sorption and availability from biochars and soil/biochar mixtures. *Clean-Soil Air Water* 42(5):626–634. <https://doi.org/10.1002/clen.201300089>
- Deng YX, Weng LP, Li YT, Chen YL, Ma J (2020) Redox-dependent effects of phosphate on arsenic speciation in paddy soils. *Environ Pollut* 264:114783. <https://doi.org/10.1016/j.envpol.2020.114783>
- Ding SM, Wang Y, Xu D, Zhu CG, Zhang CS (2013) Gel-based coloration technique for the submillimeter-scale imaging of labile phosphorus in sediments and soils with diffusive gradients in thin films. *Environ Sci Technol* 47(14):7821–7829. <https://doi.org/10.1021/es400192j>
- Eduah JO, Nartey EK, Abekoe MK, Breuning-Madsen H, Andersen MN (2019) Phosphorus retention and availability in three contrasting soils amended with rice husk and corn cob biochar at varying pyrolysis temperatures. *Geoderma* 341:10–17. <https://doi.org/10.1016/j.geoderma.2019.01.016>
- Eltohamy KM, Milham PJ, Gouda M, Menezes-Blackburn D, Khan S, Liu B, Jin J, Ye Y, Liang X (2023) Size and composition of colloidal phosphorus across agricultural soils amended with biochar manure and biogas slurry. *Carbon Res* 2:16. <https://doi.org/10.1007/s44246-023-00048-2>
- Fang W, Williams PN, Zhang H, Yang Y, Yin DX, Liu ZD, Sun HT, Luo J (2021a) Combining multiple high-resolution *in situ* techniques to understand phosphorous availability around rice roots. *Environ Sci Technol* 55(19):13082–13092. <https://doi.org/10.1021/acs.est.1c05358>

- Fang W, Yang Y, Wang HL, Yang DX, Luo J, Williams PN (2021b) Rice rhizospheric effects on the bioavailability of toxic trace elements during land application of biochar. *Environ Sci Technol* 55(11):7344–7354. <https://doi.org/10.1021/acs.est.0c07206>
- Gao S, DeLuca TH, Cleveland CC (2019) Biochar additions alter phosphorus and nitrogen availability in agricultural ecosystems: A meta-analysis. *Sci Total Environ* 654:463–472. <https://doi.org/10.1016/j.scitotenv.2018.11.124>
- Ghodszad L, Reyhanitabar A, Maghsoudi MR, Lajayer BA, Chang SX (2021) Biochar affects the fate of phosphorus in soil and water: A critical review. *Chemosphere* 283(1):131176. <https://doi.org/10.1016/j.chemosphere.2021.131176>
- Ghodszad L, Reyhanitabar A, Oustan S, Alidokht L (2022) Phosphorus sorption and desorption characteristics of soils as affected by biochar. *Soil Till. Res.* 216. <https://doi.org/10.1016/j.still.2021.105251>
- Glaser B, Lehr VI (2019) Biochar effects on phosphorus availability in agricultural soils: A meta-analysis. *Sci Rep* 9:9338. <https://doi.org/10.1038/s41598-019-45693-z>
- Jiang BS, Shen JL, Sun MH, Hu Y, Jiang WQ, Wang J, Li Y, Wu JC (2021) Soil phosphorus availability and rice phosphorus uptake in paddy fields under various agronomic practices. *Pedosphere* 31(1):103–115
- Jin ZW, Chen C, Chen XM, Jiang F, Hopkins I, Zhang XL, Han ZQ, Billy G, Benavides J (2019) Soil acidity available phosphorus content and optimal biochar and nitrogen fertilizer application rates: A five-year field trial in upland red soil China. *Field Crop Res* 232:77–87. <https://doi.org/10.1016/j.fcr.2018.12.013>
- Kappler A, Wuestner ML, Ruecker A, Harter J, Halama M, Behrens S (2014) Biochar as an electron shuttle between bacteria and Fe(III) minerals. *Environ Sci Tech* 1(8):339–344. <https://doi.org/10.1021/ez5002209>
- Khan I, Fahad S, Wu L, Zhou W, Xu P, Sun Z, Salam A, Imran M, Jiang MD, Kuzyakov Y, Hu RG (2019) Labile organic matter intensifies phosphorus mobilization in paddy soils by microbial iron (III) reduction. *Geoderma* 352:185–196. <https://doi.org/10.1016/j.geoderma.2019.06.011>
- Kreuzeder A, Santner J, Scharsching V, Oburger E, Hoefler C, Hann S, Wenzel WW (2018) *In situ* observation of localized sub-mm scale changes of phosphorus biogeochemistry in the rhizosphere. *Plant Soil* 424(1–2):573–589. <https://doi.org/10.1007/s11104-017-3542-0>
- Larsen M, Santner J, Oburger E, Wenzel WW, Glud RN (2015) O₂ dynamics in the rhizosphere of young rice plants (*Oryza sativa* L.) as studied by planar optodes. *Plant Soil* 390(1–2): 279–292. <https://doi.org/10.1007/s11104-015-2382-z>
- Li C, Ding SM, Chen MS, Sun Q, Zhang Y, Ma X, Zhong ZL, Tsang DCW, Wang Y (2022) Mechanistic insights into trace metal mobilization at the micro-scale in the rhizosphere of *Vallisneria spiralis*. *Sci Total Environ* 806:150735. <https://doi.org/10.1016/j.scitotenv.2021.150735>
- Li YH, Shahbaz M, Zhu ZK, Deng YW, Tong YY, Chen L, Wu JS, Ge TD (2021) Oxygen availability determines key regulators in soil organic carbon mineralisation in paddy soils. *Soil Biol. Biochem.* 153. <https://doi.org/10.1016/j.soilbio.2020.108106>
- Maranguit D, Guillaume T, Kuzyakov Y (2017) Effects of flooding on phosphorus and iron mobilization in highly weathered soils under different land-use types: Short-term effects and mechanisms. *CATENA* 158:161–170. <https://doi.org/10.1016/j.catena.2017.06.023>
- Marschner P, Crowley D, Rengel Z (2011) Rhizosphere interactions between microorganisms and plants govern iron and phosphorus acquisition along the root axis - model and research methods. *Soil Biol Biochem* 43(5):883–894. <https://doi.org/10.1016/j.soilbio.2011.01.005>
- McRose DL, Newman DK (2021) Redox-active antibiotics enhance phosphorus bioavailability. *Science* 371(6533):1033–1037. <https://doi.org/10.1126/science.abd1515>
- Murphy J, Riley JP (1962) A modified single solution method for the determination of phosphate in natural waters. *Anal. Chim. Acta* 27 (C) 678–681.
- Ngatila LW, Hsieh YP, Nemours D, Fu R, Taylor RW (2017) Potential phosphorus eutrophication mitigation strategy: Biochar carbon composition thermal stability and pH influence phosphorus sorption. *Chemosphere* 180:201–211. <https://doi.org/10.1016/j.chemosphere.2017.04.012>
- Pan SY, Dong CD, Su JF, Wang PY, Chen CW, Chang JS, Kim H, Huang CP, Hung CM (2021) The role of biochar in regulating the carbon phosphorus and nitrogen cycles exemplified by soil systems. *Sustainability* 13 (10) 5612. <https://doi.org/10.3390/su13105612>
- Rajendran M, Shi LZ, Wu C, Li WC, An WH, Liu ZY, Xue SG (2019) Effect of sulfur and sulfur-iron modified biochar on cadmium availability and transfer in the soil-rice system. *Chemosphere* 222:314–322. <https://doi.org/10.1016/j.chemosphere.2019.01.149>
- Ren MY, Ding SM, Dai ZH, Wang JF, Li C, Zhong ZL, Cao JX, Yang LY, Tsang DCW, Xu SW, Yang CY, Wang Y (2021) A new DGT technique comprising a hybrid sensor for the simultaneous high resolution 2D imaging of sulfides metallic cations oxyanions and dissolved oxygen. *J. Hazard Mater.* 403. <https://doi.org/10.1016/j.jhazmat.2020.123597>
- Shen JB, Yuan LX, Zhang JL, Li HG, Bai ZH, Chen XP, Zhang WF, Zhang FS (2011) Phosphorus dynamics: From soil to plant. *Plant Physiol* 156(3):997–1005. <https://doi.org/10.2307/41435013>
- Tiessen H, Moir JO (1993) Characterization of available P by sequential extraction. CRC Press
- Wang Y, Yuan JH, Chen H, Zhao X, Wang DJ, Wang SQ, Ding SM (2019) Small-scale interaction of iron and phosphorus in flooded soils with rice growth. *Sci Total Environ* 669:911–919. <https://doi.org/10.1016/j.scitotenv.2019.03.054>
- Wang QP, Liao ZY, Yao DX, Yang ZJ, Wu YH, Tang CL (2021a) Phosphorus immobilization in water and sediment using iron-based materials: A review. *Sci Total Environ* 767(1):144246. <https://doi.org/10.1016/j.scitotenv.2020.144246>
- Wang Y, Chen H, Wang L, Zhu WB, Yuan JH, Jaisi DP, Zhao X, Wang SQ (2021) Using diffusive gradients in thin films technique for *in-situ* measurement of labile phosphorus around *Oryza sativa* L. roots in flooded paddy soils. *Pedosphere* 31 (1) 76–82. [https://doi.org/10.1016/S1002-0160\(20\)60009-1](https://doi.org/10.1016/S1002-0160(20)60009-1)
- Wang LW, Deng JY, Yang XD, Hou RJ, Hou DL (2023) Role of biochar toward carbon neutrality. *Carbon Res.* 2 (2). <https://doi.org/10.1007/s44246-023-00035-7>
- Wei XM, Zhu ZK, Wei L, Wu JS, Ge TD (2019) Biogeochemical cycles of key elements in the paddy-rice rhizosphere: Microbial mechanisms and coupling processes. *Rhizosphere* 10:100145. <https://doi.org/10.1016/j.rhisph.2019.100145>
- Weihrauch C, Opp C (2018) Ecologically relevant phosphorus pools in soils and their dynamics: The story so far. *Geoderma* 325:183–194. <https://doi.org/10.1016/j.geoderma.2018.02.047>
- Williams PN, Santner J, Larsen M, Lehto NJ, Oburger E, Wenzel W, Glud RN, Davison W, Zhang H (2014) Localized flux maxima of arsenic lead and iron around root apices in flooded lowland rice. *Environ Sci Technol* 48(15):8498–8506. <https://doi.org/10.1021/es501127k>
- Wu S, Zhao YP, Chen YY, Dong XM, Wang MY, Wang GX (2019) Sulfur cycling in freshwater sediments: A cryptic driving force of iron deposition and phosphorus mobilization. *Sci Total Environ* 657:1294–1303. <https://doi.org/10.1016/j.scitotenv.2018.12.161>
- Wu MZ, Liu JD, Gao B, Sillanpaa M (2021) Phosphate substances transformation and vivianite formation in P-Fe containing sludge during the transition process of aerobic and anaerobic conditions. *Bioresour Technol* 319:124259. <https://doi.org/10.1016/j.biortech.2020.124417>
- Xu G, Zhang Y, Sun JN, Shao HB (2016) Negative interactive effects between biochar and phosphorus fertilization on phosphorus availability and plant yield in saline sodic soil. *Sci Total Environ* 568:910–915. <https://doi.org/10.1016/j.scitotenv.2016.06.079>
- Xu XW, Wang P, Zhang J, Chen C, Wang ZP, Kopittke PM, Kretzschmar R, Zhao FJ (2019) Microbial sulfate reduction decreases arsenic mobilization in flooded paddy soils with high potential for microbial Fe reduction. *Environ Pollut* 251:952–960. <https://doi.org/10.1016/j.envpol.2019.05.086>
- Yang CD, Lu SG (2022) The dynamic changes of phosphorus availability in straw/biochar-amended soils during the rice growth revealed by a combination of chemical extraction and DGT technique. *J Soil Sediment* 22(3):957–967. <https://doi.org/10.1007/s11368-021-03131-6>
- Yang XY, Chen XW, Yang XT (2019) Effect of organic matter on phosphorus adsorption and desorption in a black soil from Northeast China. *Soil Till Res* 187:85–91. <https://doi.org/10.1016/j.still.2018.11.016>
- Yang L, Wu YC, Wang YC, An WQ, Jin J, Sun K, Wang XK (2021) Effects of biochar addition on the abundance speciation availability and leaching loss of soil phosphorus. *Sci Total Environ* 758:143657. <https://doi.org/10.1016/j.scitotenv.2020.143657>
- Yin DX, Fang W, Guan DX, Williams PN, Moreno-Jimenez E, Gao Y, Zhao FJ, Ma LQ, Zhang H, Luo J (2020) Localized intensification of arsenic release within the emergent rice rhizosphere. *Environ Sci Technol* 54(6):3138–3147. <https://doi.org/10.1021/acs.est.9b04819>

- Yuan HZ, Tai ZQ, Li Q, Liu EF (2020) *In-situ* high-resolution evidence from water-sediment interface for significant role of iron bound phosphorus in eutrophic lake. *Sci Total Environ* 706:136040. <https://doi.org/10.1016/j.scitotenv.2019.136040>
- Yuan HZ, Wang HX, Zhou YW, Jia BC, Yu JH, Cai YW, Yang Z, Liu EF, Li Q, Yin HB (2021) Water-level fluctuations regulate the availability and diffusion kinetics process of phosphorus at lake water-sediment interface. *Water Res* 200:117258. <https://doi.org/10.1016/j.watres.2021.117258>
- Zhang YS, Lin XY, Werner W (2003) The effect of soil flooding on the transformation of Fe oxides and the adsorption/desorption behavior of phosphate. *J Plant Nutr Soil Sc* 166(1):68–75. <https://doi.org/10.1002/jpln.200390014>
- Zhou CF, Heal K, Tigabu M, Xia LD, Hu HY, Yin DY, Ma XQ (2020) Biochar addition to forest plantation soil enhances phosphorus availability and soil bacterial community diversity. *Forest Ecol Manag* 455:115635. <https://doi.org/10.1016/j.foreco.2019.117635>

Publisher's Note

Springer Nature remains neutral with regard to jurisdictional claims in published maps and institutional affiliations.